Institut für Theoretische Physik

Universität Würzburg

M.N.Kiselev

Ginzburg-Landau functional for nearly AFM perfect and disordered Kondo lattices

In collaboration with K.Kikoin, R.Oppermann

Outline

- Criticality in HF compounds
- Kondo Lattice Model
- AFM and Spin Liquid instabilities
- Spin Glass transition
- Doniach’s Diagram revisited
- Correlations between Kondo clouds
- Conclusions

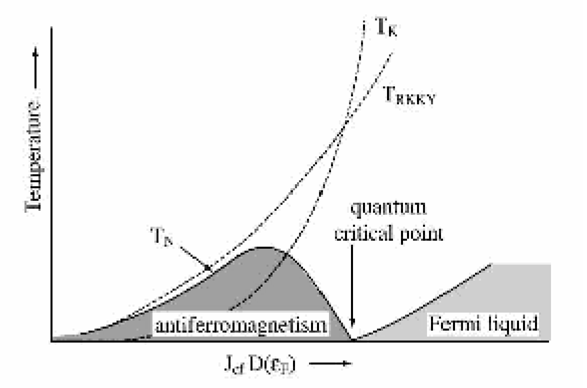

References:

M.Kiselev and R.Oppermann, Schwinger-Keldysh Semionic Approach for Quantum Spin Systems. Phys. Rev. Lett. **85**, 5631 (2000)
M.Kiselev, H.Feldmann and R.Oppermann, Semi-fermionic representation of SU(N) Hamiltonians. Eur. Phys. J. **B 22**, 53 (2001)
M.Kiselev, K.Kikoin and R.Oppermann, Ginzburg-Landau functional for nearly Antiferromagnetic perfect and disordered Kondo lattices. Phys. Rev. **B 65**, 184410 (2002)
M.Kiselev, K.Kikoin, JMMM (2004)

Competition between Kondo and AFM order in heavy fermion compounds

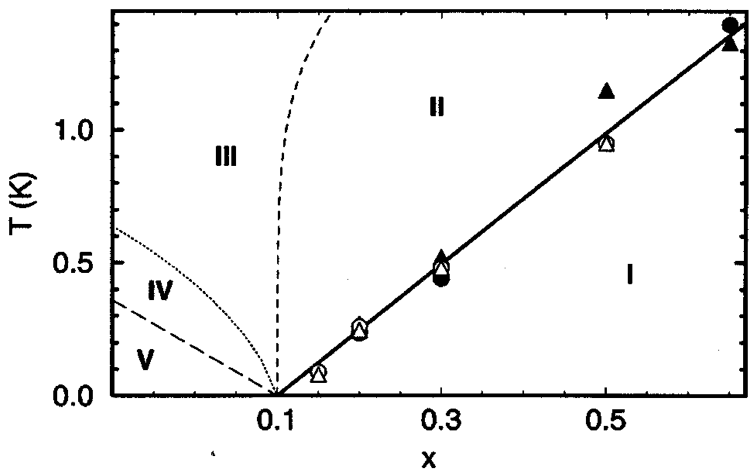

FIG. 1. Phase diagram of $CeCu_{6-x}Au_x$. The points are Néel temperatures [7] (open and closed symbols for single and polycrystals, respectively), the solid line denotes the phase transition, the dashed lines are theoretical crossover lines. The regions are described in the text.

A.Rosch et al.PRL 79,159 (1997)

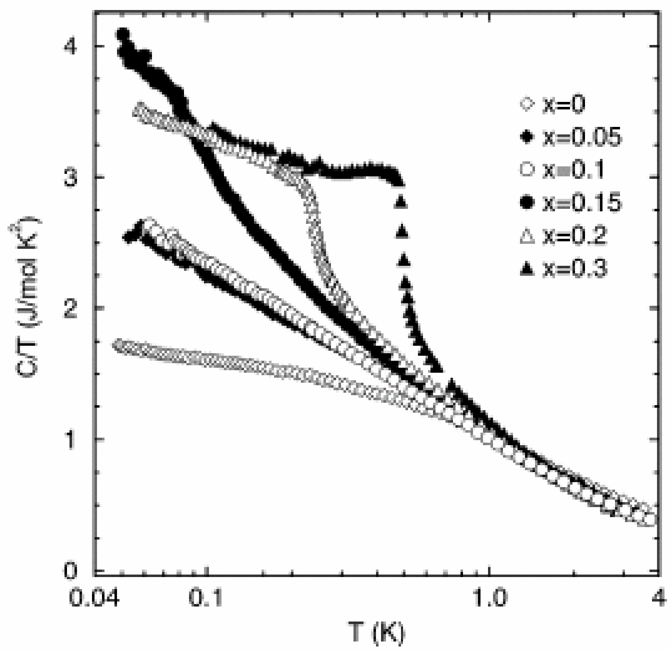

FIG. 2. The specific heat C/T of $CeCu_{6-x}Au_x$ (from [7]) on a logarithmic scale.

Non-Fermi Liquid behavior
in the vicinity of QCP

Disordered Kondo systems

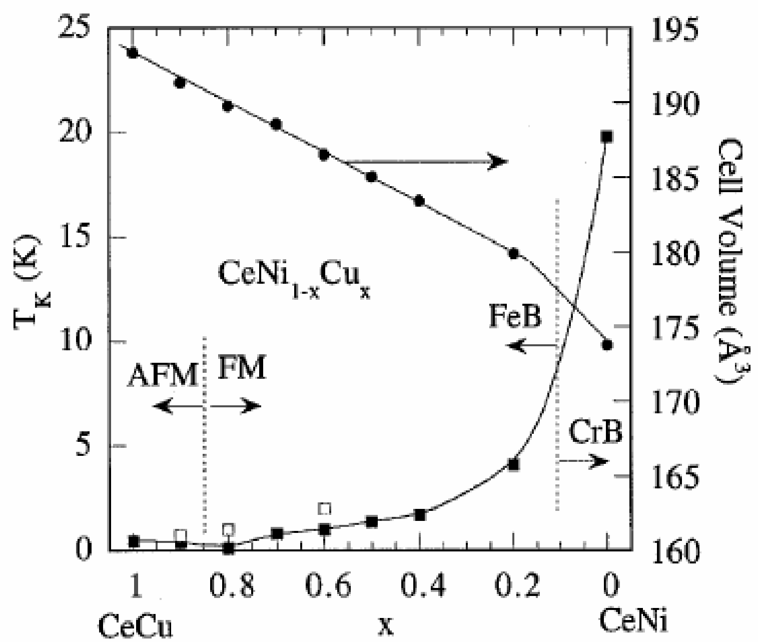

FIG. 1. Concentration dependence of the cell volume (full circles) and the Kondo temperature estimated from different techniques: magnetic susceptibility ($|\theta_p|/10$, full squares), quasielastic neutron scattering (QENS, open squares) for the CeNi$_{1-x}$Cu$_x$ series. The broken lines separate the FeB-CrB crystallographic structures and AFM-FM magnetic states. Full lines are guides for the eyes.

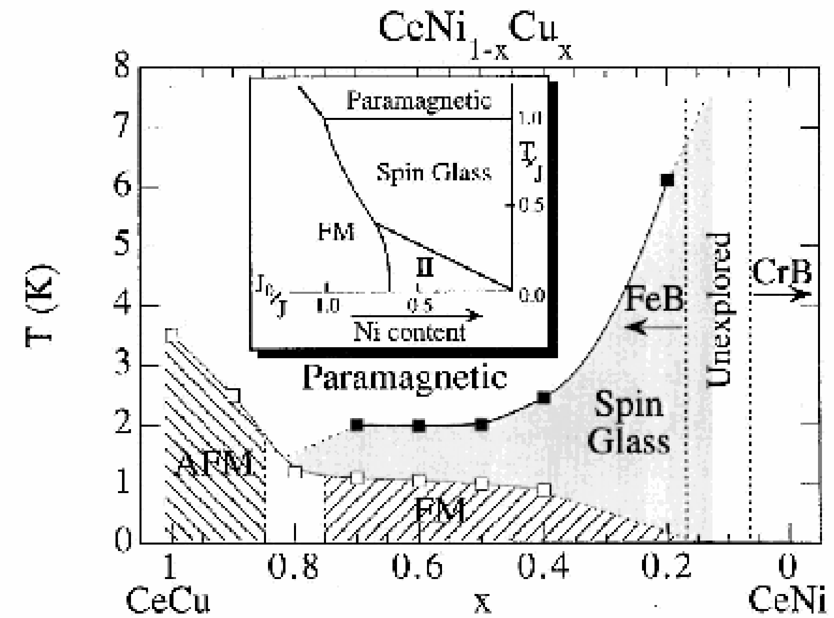

FIG. 4. Magnetic phase diagram for the CeNi$_{1-x}$Cu$_x$ series as a function of Cu concentration, where open squares represent the long-range magnetic ordering temperature $T_{C,N}$ and full squares represent the spin-glass freezing temperature T_f. Inset: Van Hemmen classical phase diagram proposed in Ref. 19. The arrow shows the direction of the displacement for increasing Ni content to help the comparison with the experimental diagram.

J.Garsia Soldevilla et al. PRB 61, 6821 (2000)

Interplay between Kondo effect and Spin Glass correlations

Non-Fermi-Liquid behavior

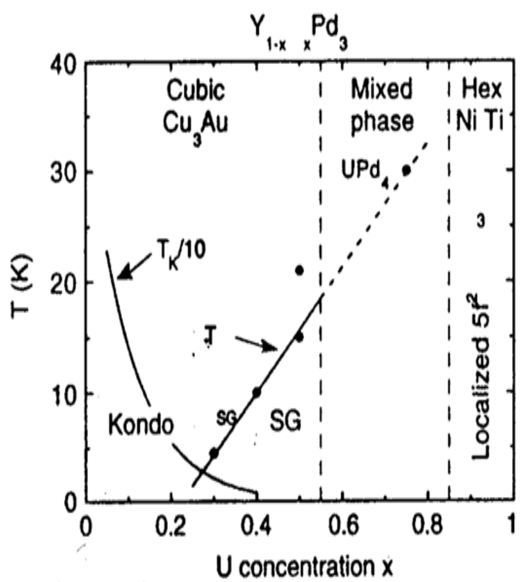

Fig. 1. Low temperature - U concentration phase diagram of $Y_{1-x}U_xPd_3$. From Ref. 2.

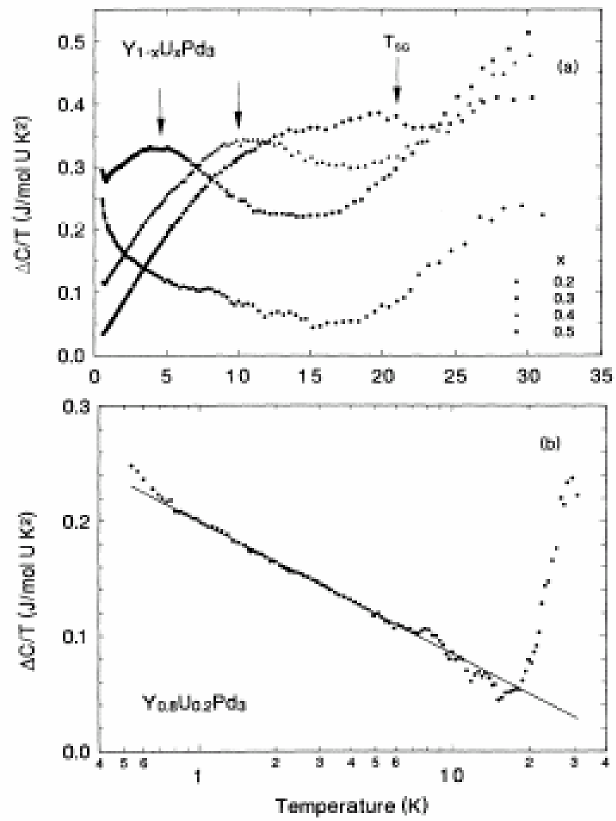

FIG. 2. (a) Temperature dependence of the electronic specific heat per U, $\Delta C(T)/T$ vs T, for $Y_{1-x}U_xPd_3$, $0.2 \leq x \leq 0.5$. T_{SG} is the peak position of $\Delta C(T)/T$ associated with apparent spin-glass freezing; $\chi(T)$ shows an onset to irreversibility at the same temperature. Note (i) the lack of a peak for $x = 0.2$, and (ii) the upturn near 20 K due to an apparent excited-state Schottky anomaly. (b) $\Delta C(T)/T$ vs $\ln T$ for $Y_{0.8}U_{0.2}Pd_3$. The solid line represents a least-squares fit of the data by the form $-(0.25/T_K)\ln(T/0.41T_K)+b$ [9]. From the slope we obtain $T_K = 42$ K, and the background coefficient b is 61 mJ/mol K², which likely arises from an excited-state Schottky anomaly.

M.B.Maple et al, JLTP 1995
C.L.Seaman et al, PRL 1991

Competition between AFM and Spin Glass

de Almeida – Thouless Line

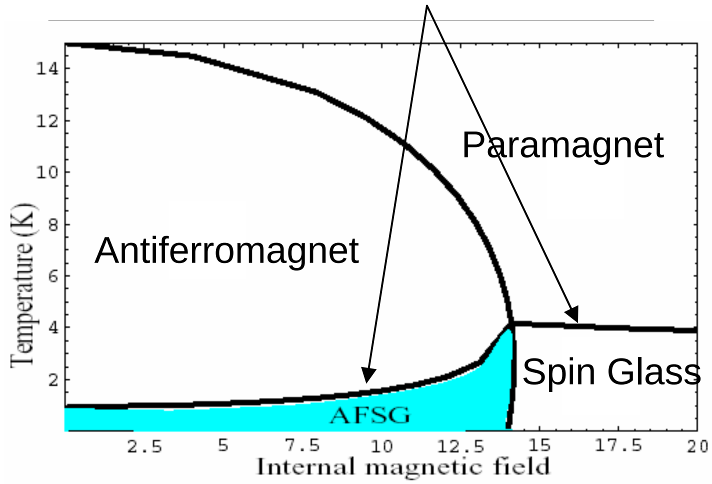

Non-ergodic Spin Glass
Shender, Korenblit 1986

$$Ce_2Au_{1-x}Co_xSi_3$$

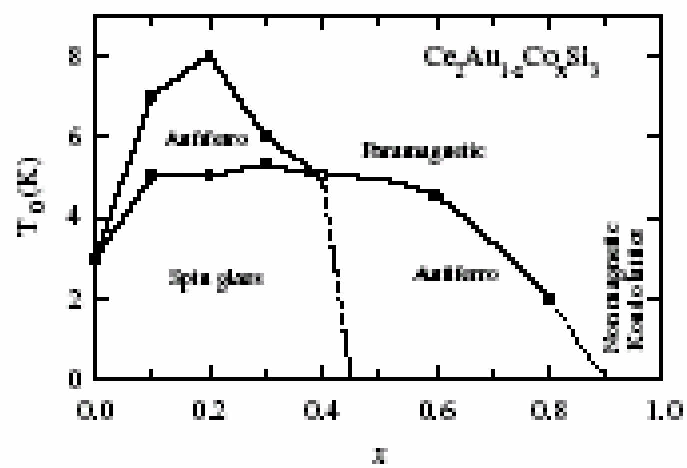

Fig. 3. Schematic representation of the magnetic phase diagram of the alloy series, $Ce_2Au_{1-x}Co_xSi_3$. T_0 represents magnetic transition temperature. The continuous lines through the data points serve as a guide to the eyes.

Doniach's diagram evolution (1977-2004)

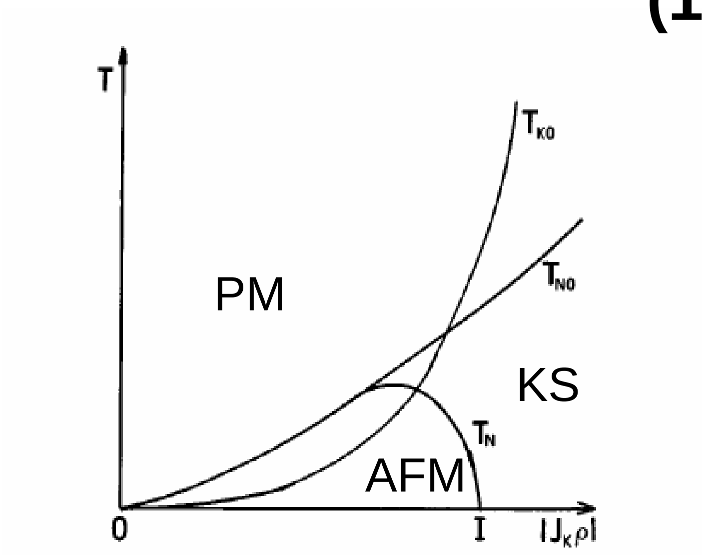

FIG. 1. Doniach diagram: Plot of the Néel and Kondo temperatures as a function of $|J_K\rho|$, as explained in text.

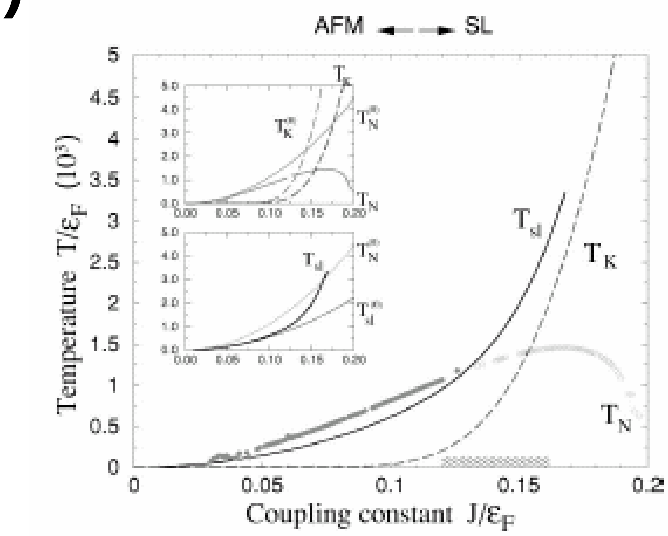

MNK et al PRB 2002

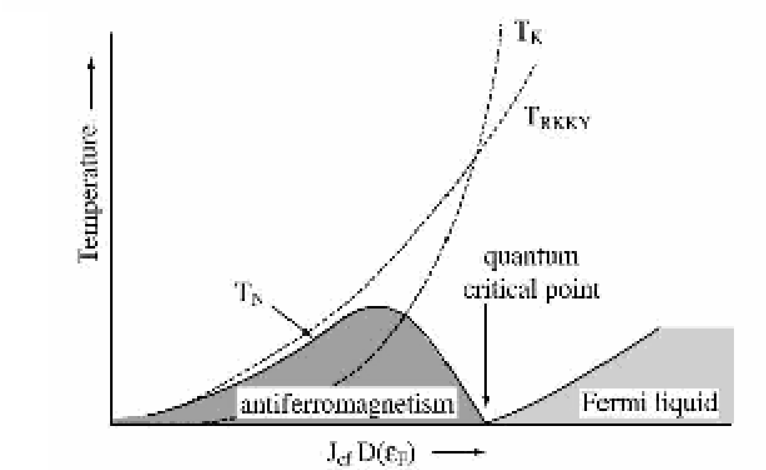

Y.Onuki et al,Physica B 2001

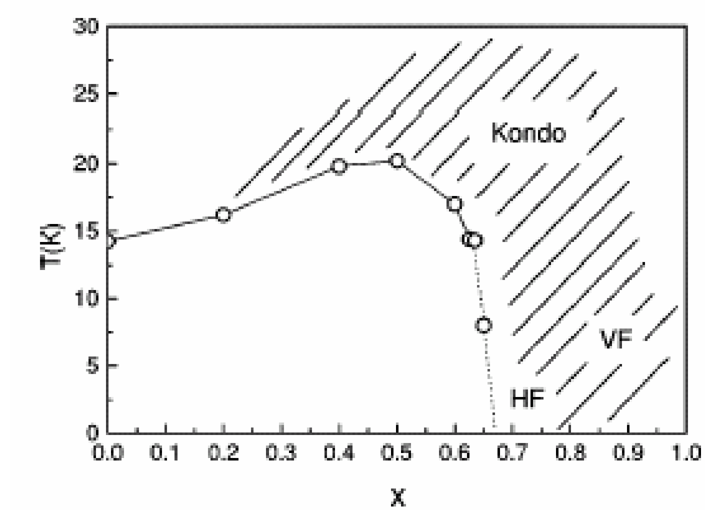

Z.Housain et all, PRB 2004

Magnetic and Kondo correlations in Kondo Lattices

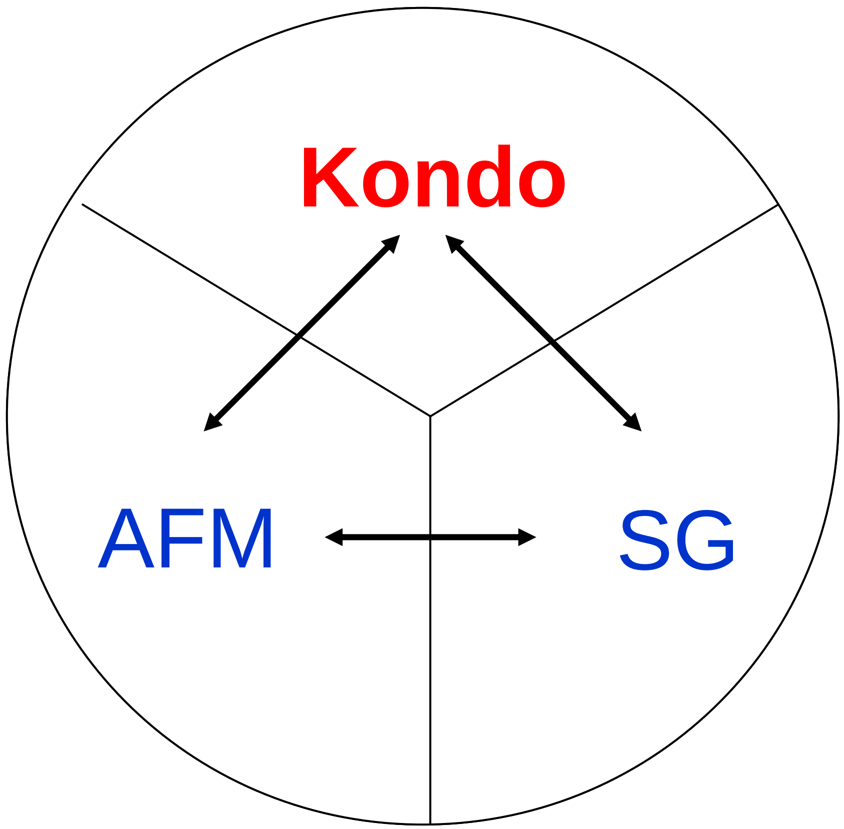

Single impurity Kondo effect

Kondo screening

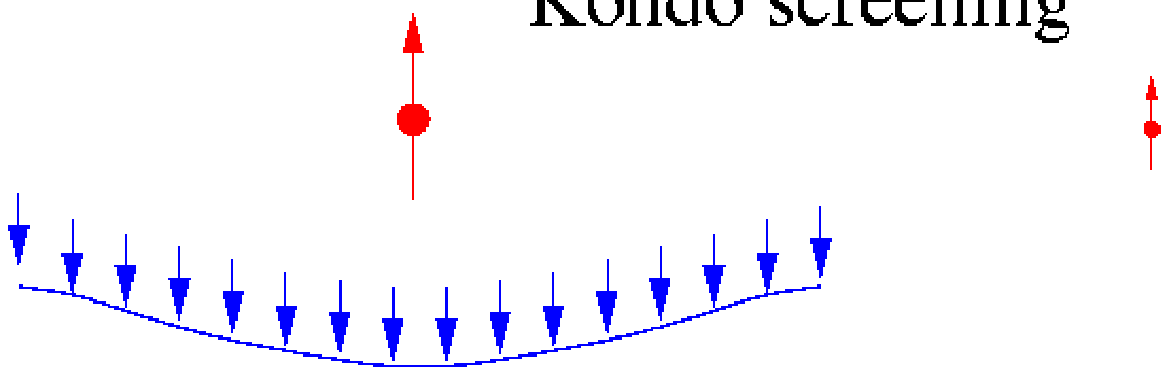

Short range order

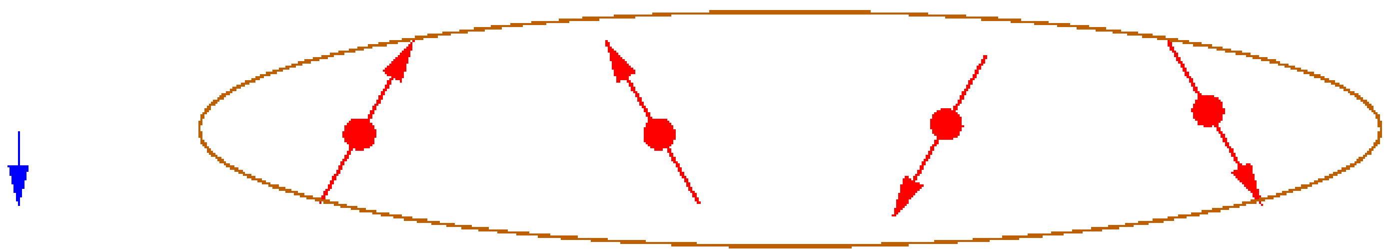

Kondo Cloud

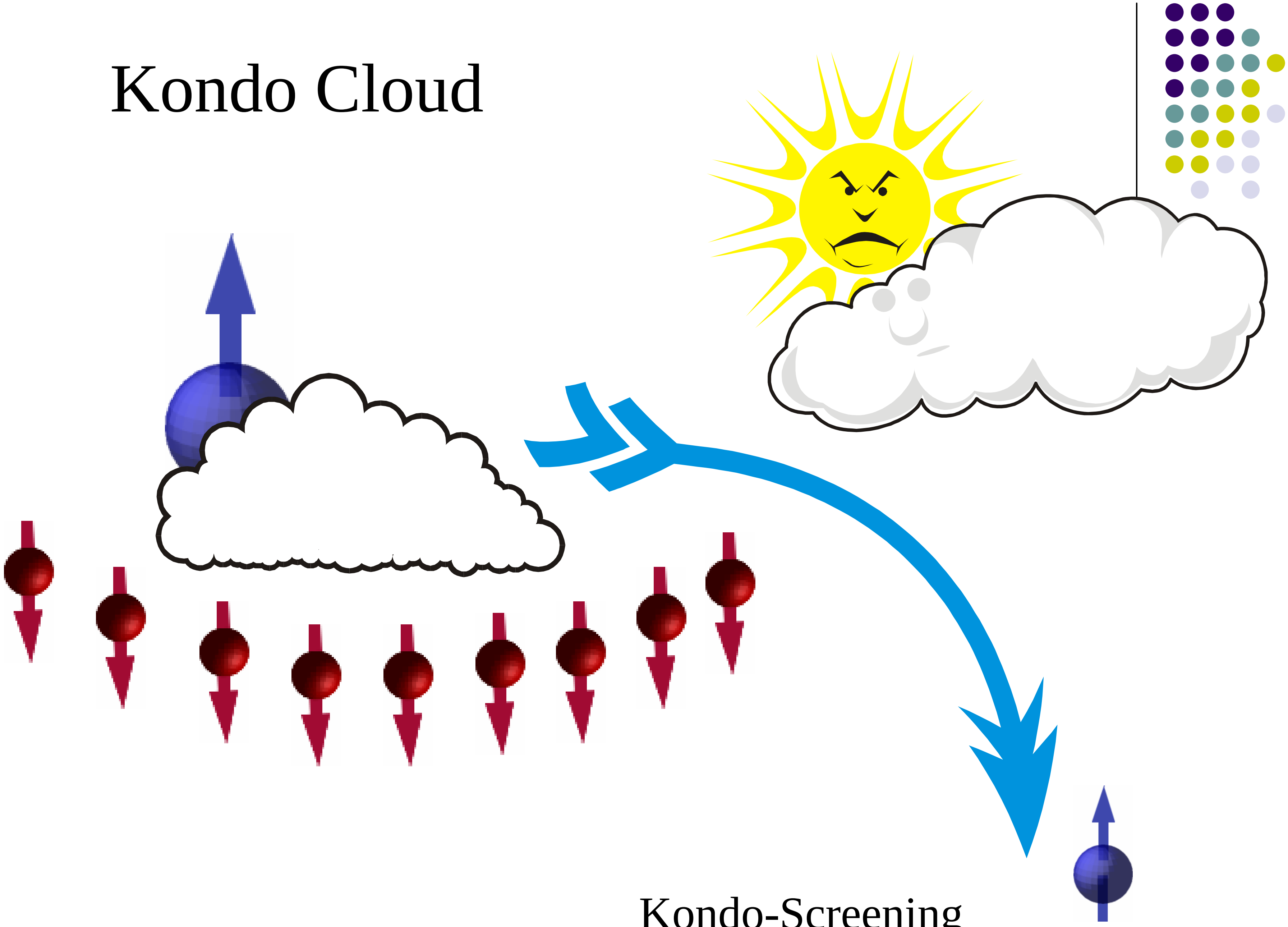

Model

$$H = \sum_k \varepsilon(k) c^{+}_{k,\sigma} c_{k,\sigma} + J \sum_i \vec{S}_i \vec{s}_i + \sum_{ij} I_{ij} \vec{S}_i \vec{S}_j$$

d-electrons Kondo RKKY

$$I_{ij} = I^{RKKY} = -\left(\frac{J^2}{\varepsilon_F}\right) \frac{\cos\left[2k_F R_{ij} - \pi(d+1)/2 + \delta(R_{ij})\right]}{(2k_F R_{ij})^d}$$

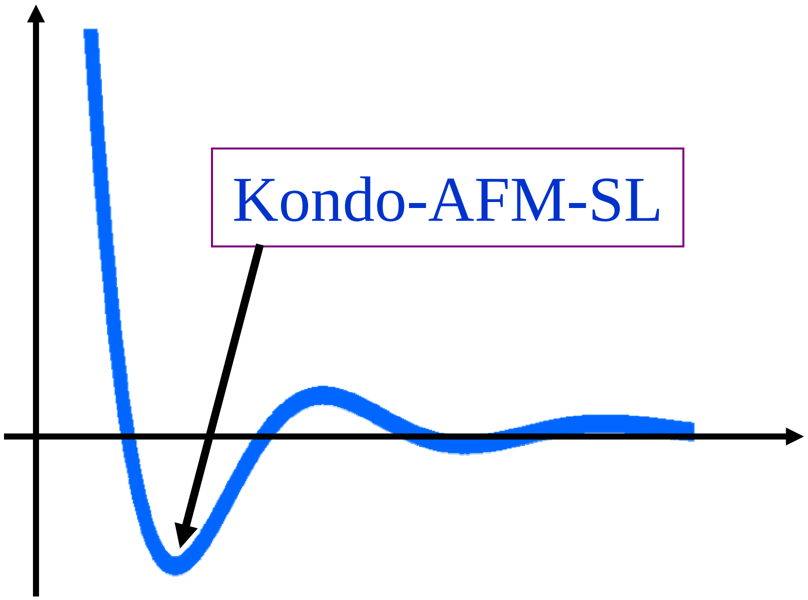

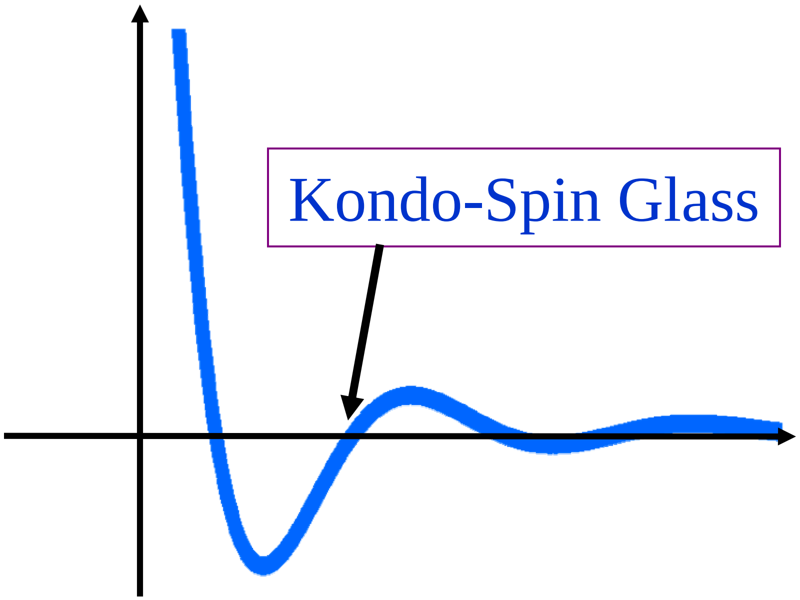

Methods

Semi-fermionic representation

$$\vec{S} = f^{+}_{\alpha} \vec{\tau}_{\alpha\beta} f_{\beta}$$

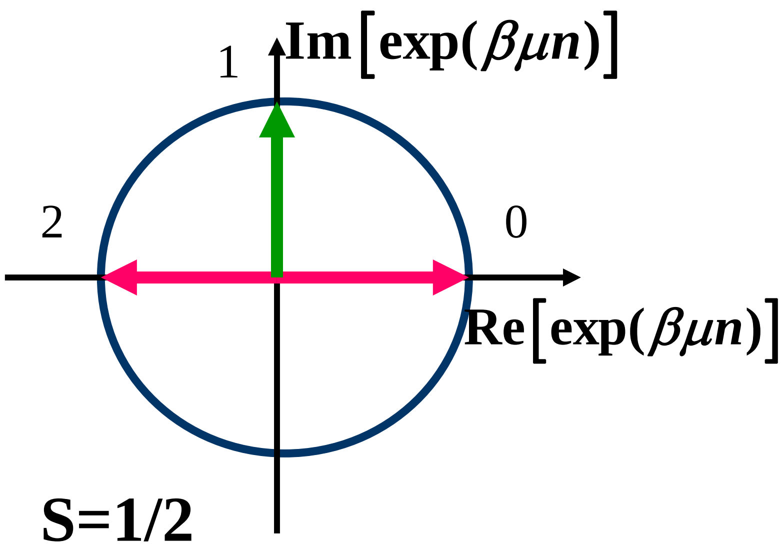

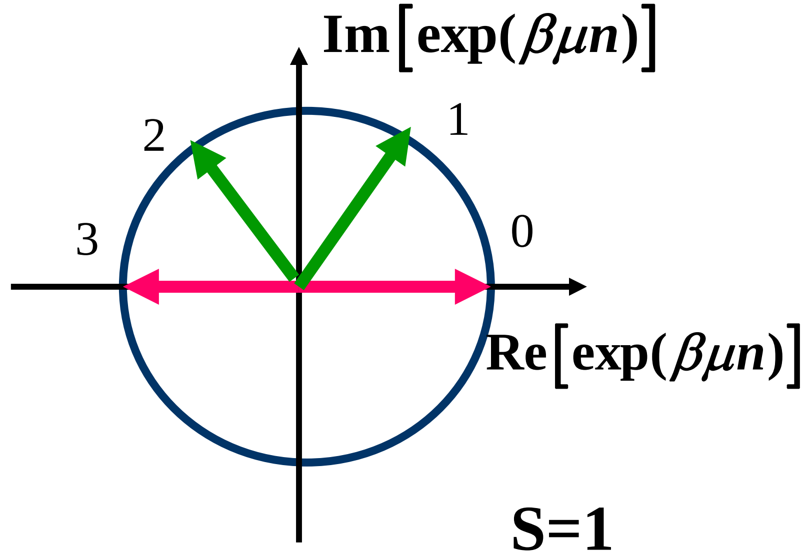

$$\omega = 2\pi T\left(n + 1/4\right)$$

$$\omega = 2\pi T\left(n + 1/3\right)$$

$$\mu = -i\frac{\pi T}{2S+1}$$

$$Z_S = Tr\left[\exp\left(-\beta H_S\right)\right] = ATr\left[\exp\left(-\beta H_F + \beta\mu N_F\right)\right]$$

Ginzburg-Landau functional for KL model

Program:

- **Represent spins in terms of semi-fermions**
- **Integrate out the highest energies**
- **Introduce effective bosonic fields responsible for magnetic (spin glass, spin liquid) correlations**
- **Introduce effective „semi-bosonic“ fields describing Kondo correlations**
- **Calculate a free energy taking into account Kondo corrections, construct Ginzburg-Landau functional**
- **Derive new saddle point equations for magnetic (SL) transitions**
- **Include fluctuations**

Advantages of semi-fermionic techniques

Proper accounts for spin statistics (no local constraint)

Correctly describes Kondo effect (no “Kondo condensate”)

GL functional near AFM transition point

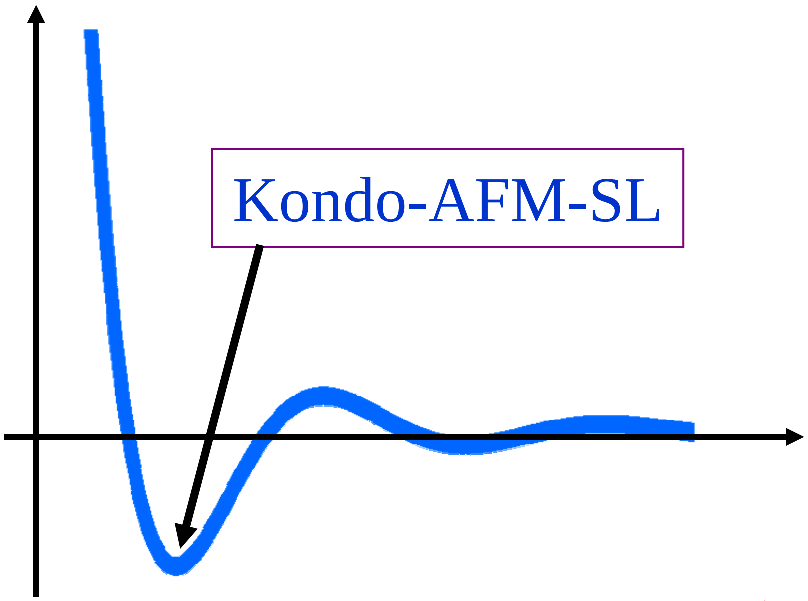

$$I_{ij} = I^{RKKY} = -\left(\frac{J^2}{\varepsilon_F}\right)\frac{\cos\left[2k_F R_{ij} - \pi\left(d+1\right)/2\right]}{(2k_F R_{ij})^d}$$

$$\beta F_{N,\Delta} = \frac{\beta\,|\,I\,|\,zN^2}{4}\tau_N + c_N N^4 + \frac{\beta\,|\,I\,|\,z\Delta^2}{2} + c_{sl}\Delta^4$$

Notations: N-Neel, Δ - Spin Liquid, q – Spin Glass, ϕ - Kondo, $\tau_\alpha = 1 - \frac{T_\alpha}{T}$

Spin Liquid

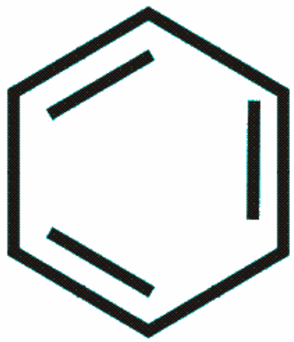

Resonating Valence Bonds

$$\Delta = -\sum_{\mathbf{q}} \nu(\mathbf{q}) \tanh\left(\frac{I_{\mathbf{q}}\Delta}{T}\right)$$

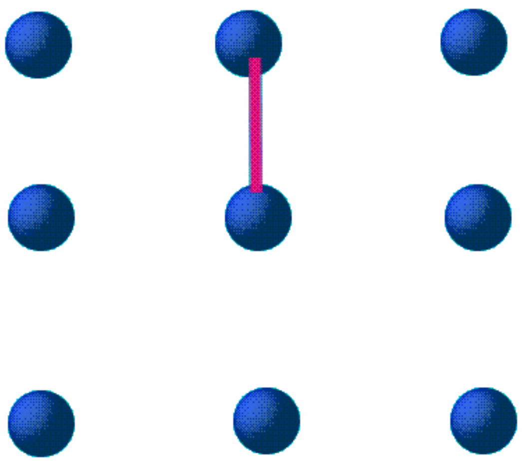

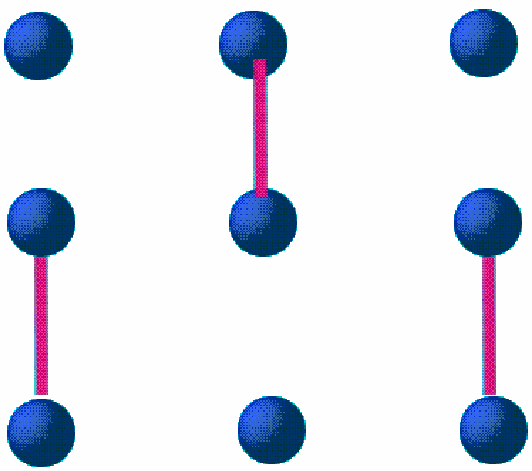

Antiferromagnetic transition

$$A_N = \sum_{q,n} \left[\frac{1}{J} - \Pi(N,q) \right] \left| \phi(q) \right|^2 - Tr \frac{1}{J_Q} N_Q N_{-Q}$$

$$N = \tanh\left(\frac{I_Q N}{2T} \right) \left[1 - \frac{a_N}{\ln(T/T_K)} \frac{\cosh^2\left(I_Q N / 2T \right)}{\cosh^2\left(I_Q N / T \right)} \right]$$

Local-field corrections reduce the Neel temperature

Kondo screening suppresses AFM transition

RVB spin liquid crossover

$$A_{\Delta} = \sum_{q,n} \left[\frac{1}{J} - \Pi(\Delta, q) \right] \left| \phi(q) \right|^2 - Tr \frac{1}{J_{p-k}} \Delta_p \Delta_k$$

$$\Delta = \sum_q \nu(q) \left[\tanh\left(\frac{I_q \Delta}{T} \right) + a_{sl} \frac{I_q \Delta}{T \ln(T / T_K)} \right]$$

Kondo „antiscreening“ effectively decreeses SL free energy

Kondo scattering favors crossover to SL state

Doniach's diagram revisited

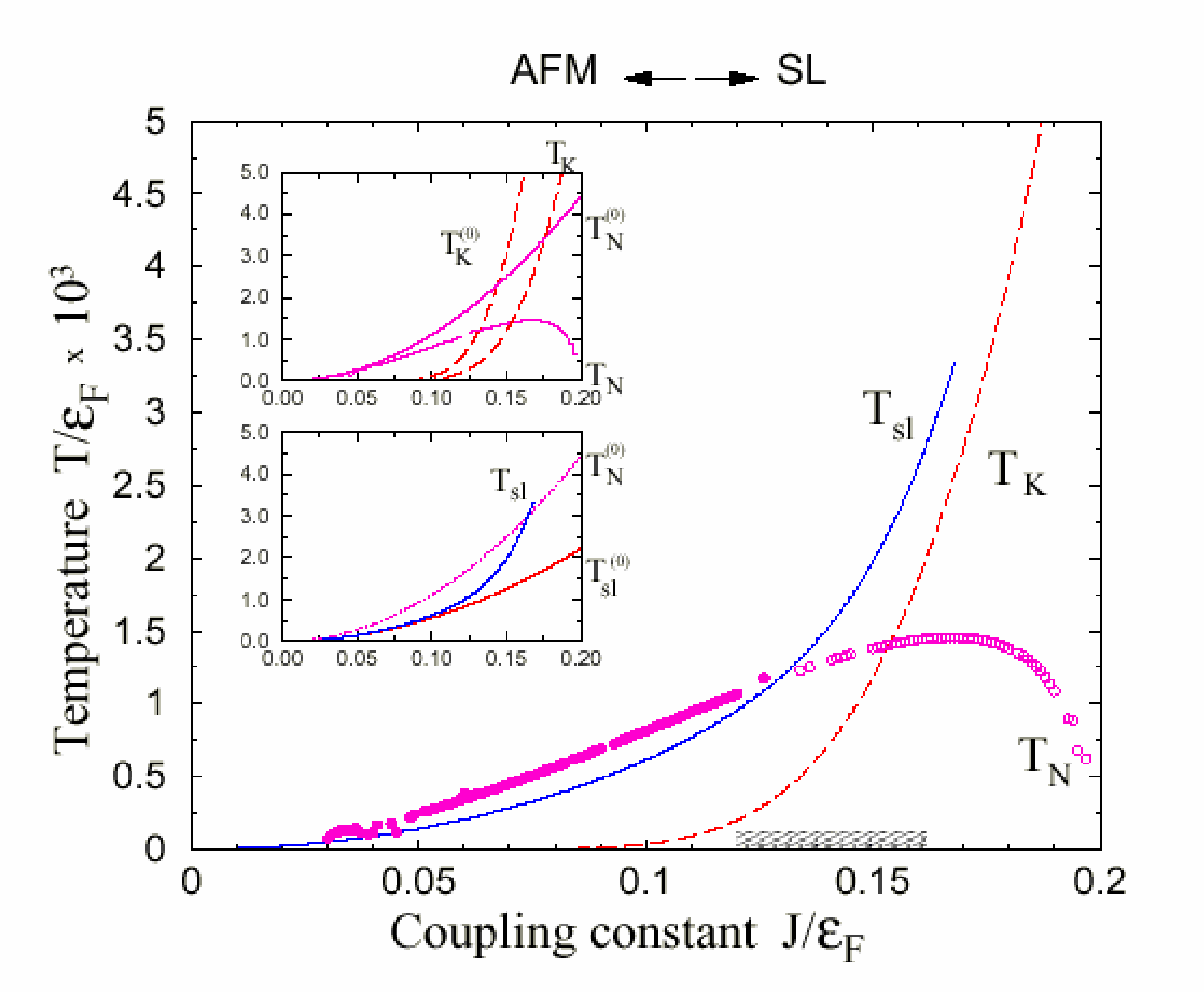

GL functional near Spin Glass transition point

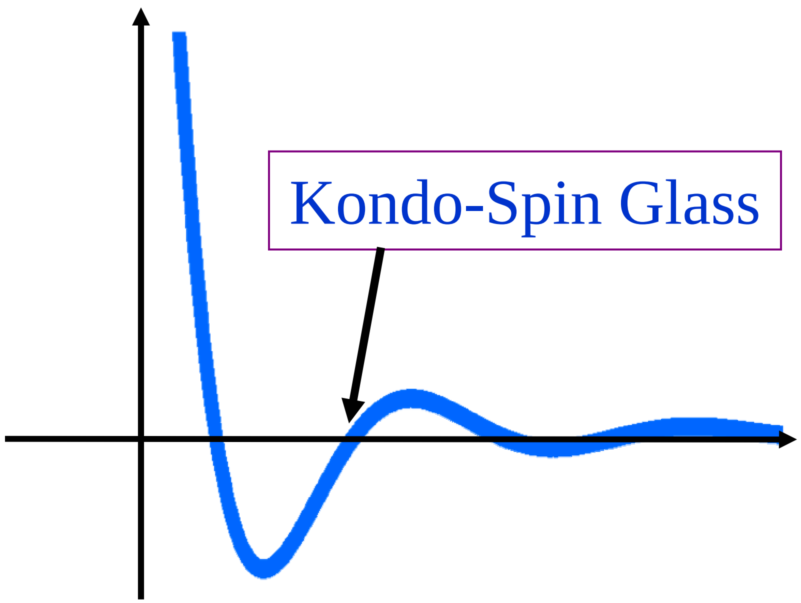

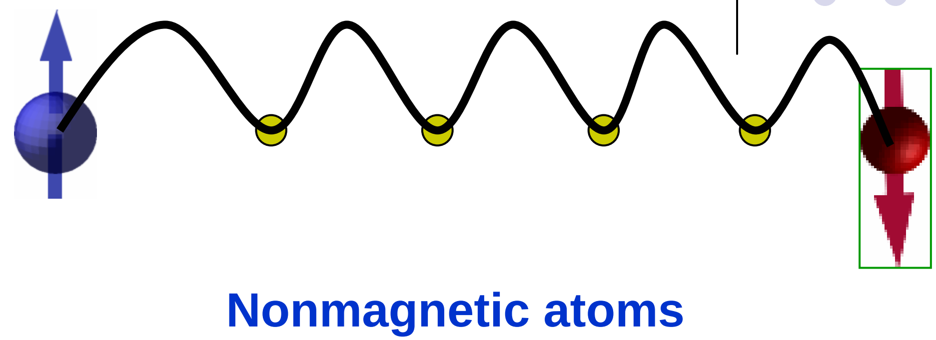

Random phase shift

$$I_{ij} = I^{RKKY} = -\left(\frac{J^2}{\varepsilon_F}\right)\frac{\cos\left[2k_F R_{ij} - \pi\left(d+1\right)/2 + \delta(R_{ij})\right]}{(2k_F R_{ij})^d}$$

$$\beta F_{SG} = \frac{z(\beta I)^2}{4} q^2 \tau_{SG} - c_{SG} q^3 + d_{SG} q^4$$

Notations: N-Neel, Δ - Spin Liquid, q – Spin Glass, ϕ - Kondo, $\tau_\alpha = 1 - \frac{T_\alpha}{T}$

Spin glass transition

$$q = \int_z^G \tanh^2\left(\frac{Iz\sqrt{q}/T}{1+2c_{sg}\left(I/T\right)^2(\bar{q}-q)/\ln\left(T/T_K\right)}\right)$$

$$q_{EA} = \left\langle S_i^a(0)S_i^b(t\to\infty)\right\rangle \qquad \bar{q} = 1 - \frac{c_{sg}}{\ln(T/T_K)}$$

Local correlations reduce the spin-glass transition temperature

Kondo scattering screens Edwards-Anderson order parameter

Interplay between Kondo effect and SG transition

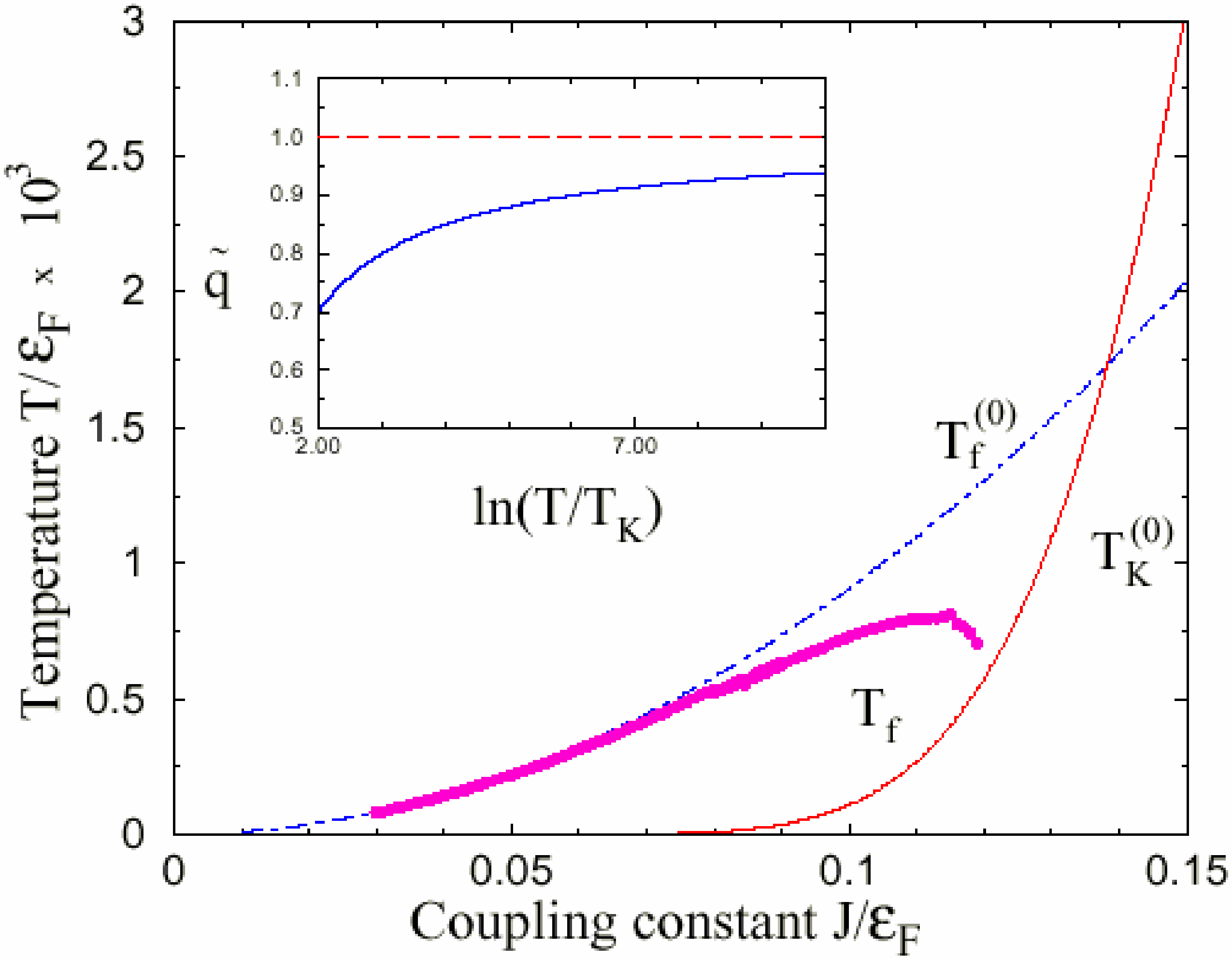

Interplay between AFM and SG transitions

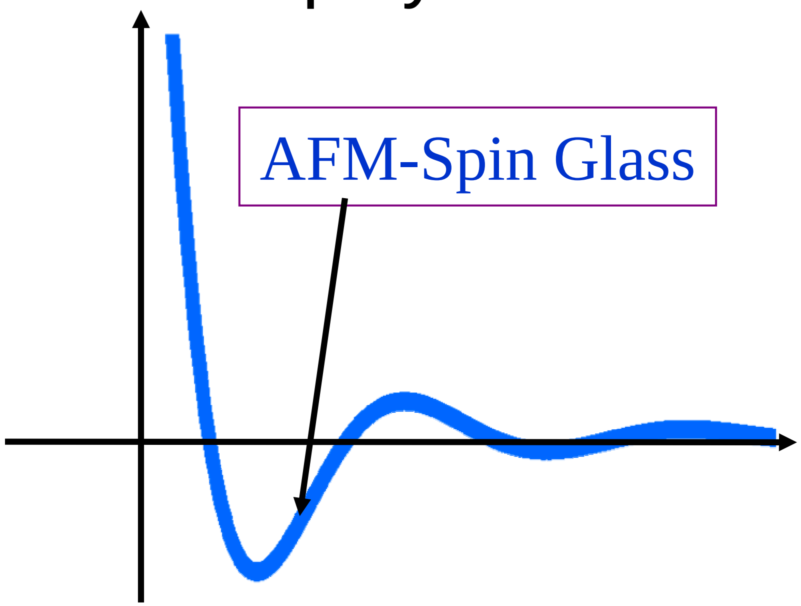

- Kondo effect is absent
- Ising-like interaction between spins
- Large coordination number (long-range interaction)

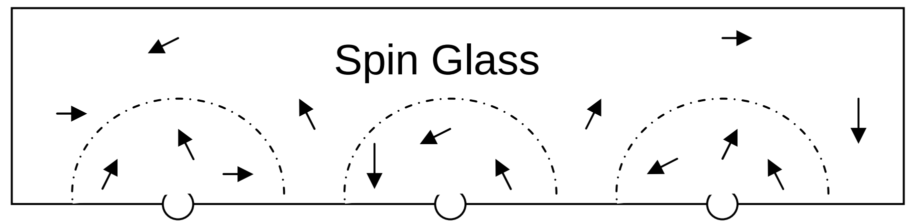

$$H = -\sum_{ij} I_{ij} S_i^z S_j^z$$

$$P(I_{ij}) \propto \exp\left[-\left(I_{ij} - \bar{I}\right)^2 N/(2I_0^2)\right]$$

$$\mathcal{H} = -\sum_{i_1=1}^{N_S}\sum_{j_2=1}^{N_S} J(r_{i_1}, r_{j_2}) S(r_{i_1}) S(r_{i_2}) - \frac{J_K}{2N_1}\sum_{l=1}^{N_p}\sigma(R_l)\sum_{i_1,i_2=1}^{N_1}\left[S(R_l + r_{i_1}) + S(R_l + r_{i_2})\right]$$
$$-H\sum_{l=1}^{N_p}\sum_{i_1,1_2=1}^{N_S}\left[\sigma(R_l) + S(R_l + r_{i_1}) + S(R_l + r_{i_2})\right] - \frac{1}{N_p}\sum_{l=1}^{N_p}\sum_{k=1}^{N_p} J_{h-k}\sigma(R_l)\sigma(R_{l+k}) - \sum_{l=1}^{N_p}\mu_h\, n(R_l).$$

Stability of Replica-symmetric solution

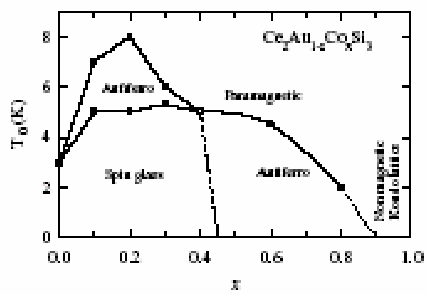

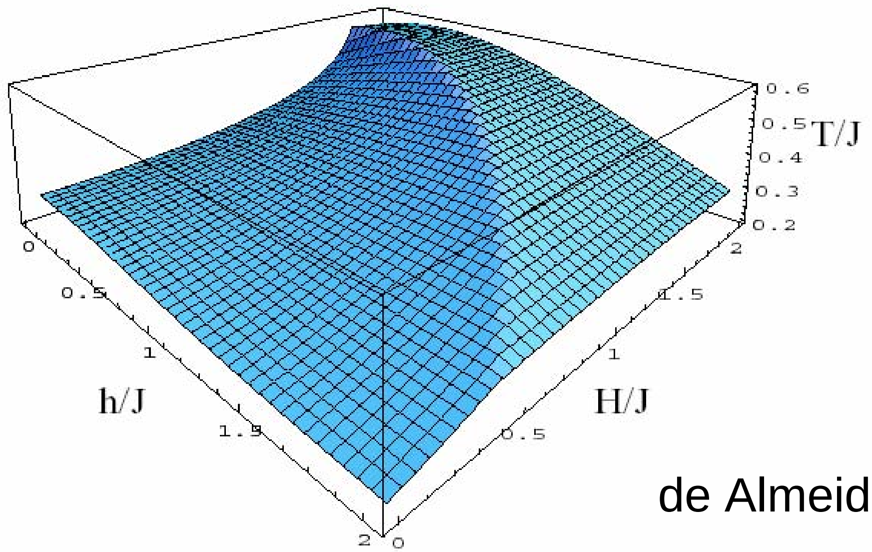

AT-surface

de Almeida – Thouless Line

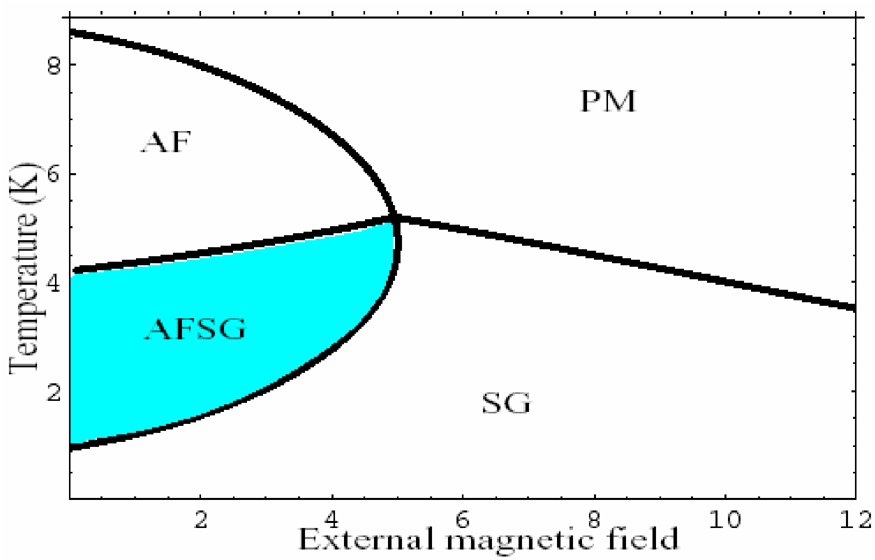

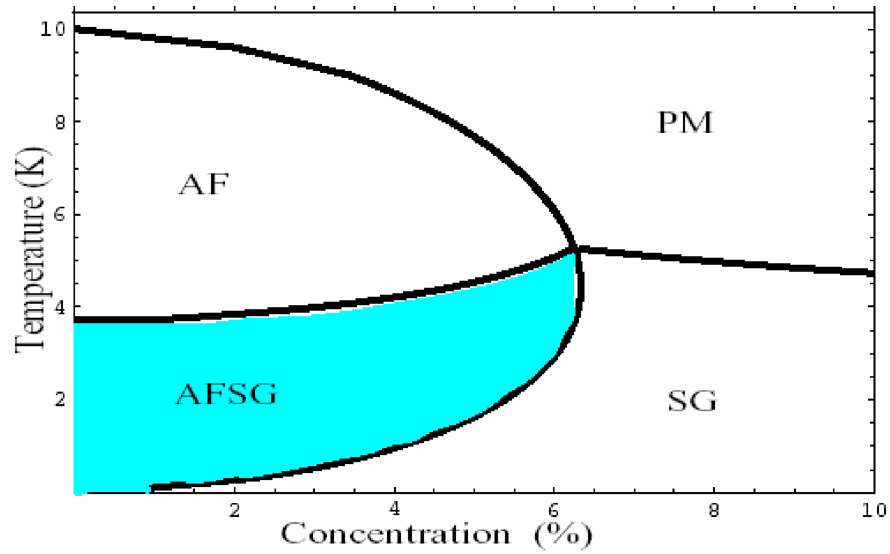

Electron-mediated correlations between Kondo Clouds

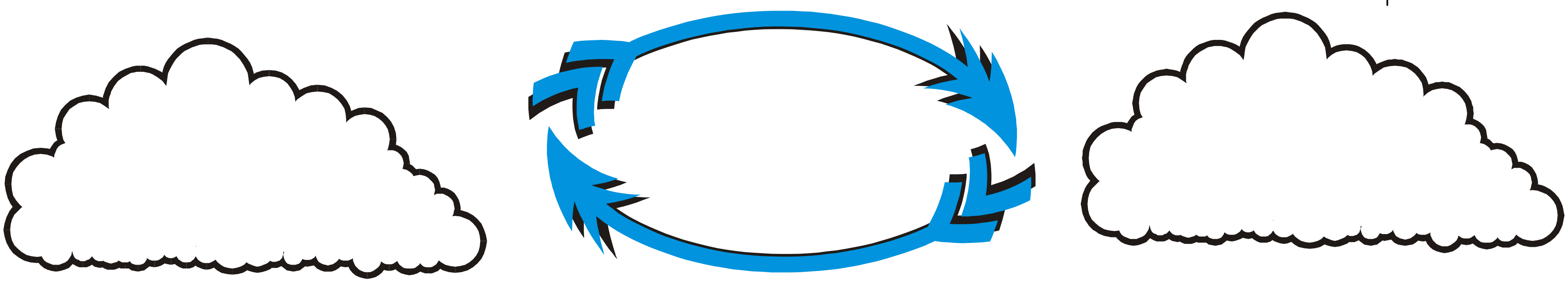

- dynamical effects far beyond mean-field description
- magnetically ordered Kondo Clouds
- universality vs. non-universality

Overlap between Kondo Clouds

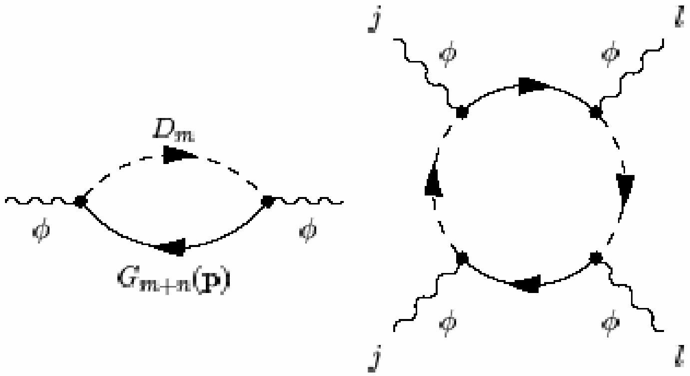

FIG. 1. Feynman diagrams describing the Kondo cloud (a) and interaction between clouds centered at different sites (b).

$$\Pi_4 \sim \frac{1}{T\varepsilon_F^2}\frac{\cos\left(2k_F R-(d-1)\pi/2\right)}{\left(2k_F R\right)^{d-1}}$$

$$K(q,\omega)=\left\langle \phi_{q,\omega}\phi_{q,\omega}\right\rangle$$

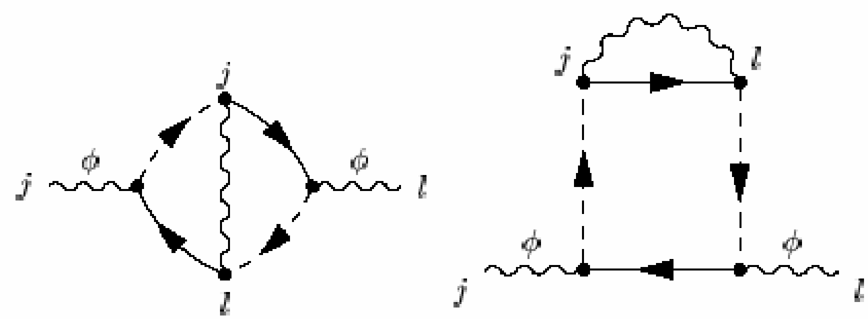

FIG. 2. Feynman diagrams for nonlocal excitations associated with the overlap of Kondo clouds.

Beyond the mean-field

$$K_{loc}^{-1}(\omega) = \frac{-i\omega}{\gamma T} + \ln\left(\frac{\{T,\omega\}}{T_K}\right)$$

$$K^{-1}(q,\omega) = K_{loc}^{-1}(\omega) + \alpha q^2$$

$$\chi^{-1}(T) = \Theta + T^{\lambda}$$

$$\lambda = \lambda(\varepsilon_F, R)$$

Critical exponents are non-universal

Local and nonlocal corrections to magnetic susceptibility

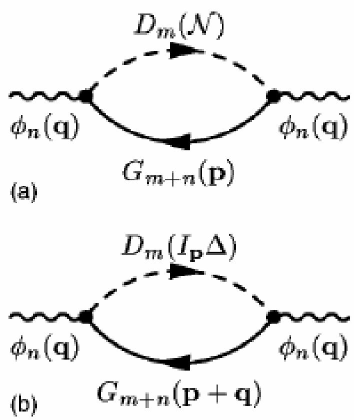

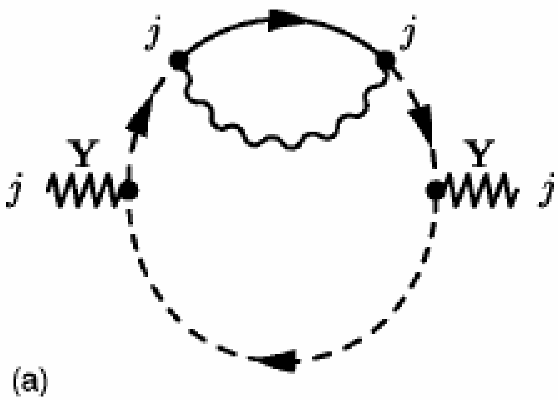

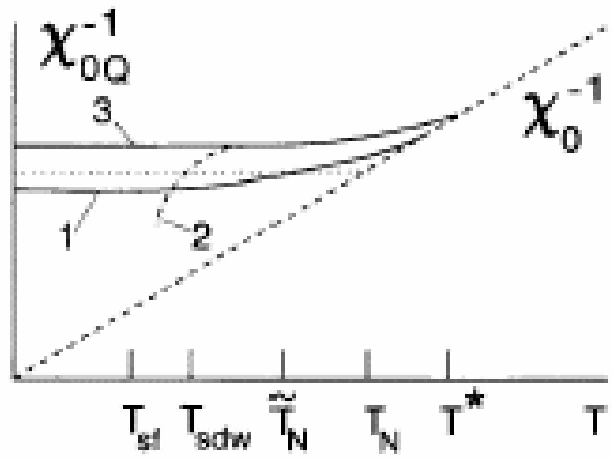

Fig. 1. Static magnetic susceptibility of RVB spin liquid.

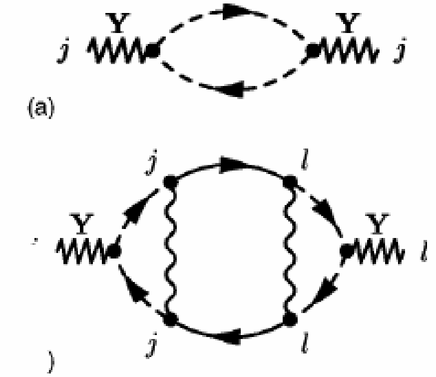

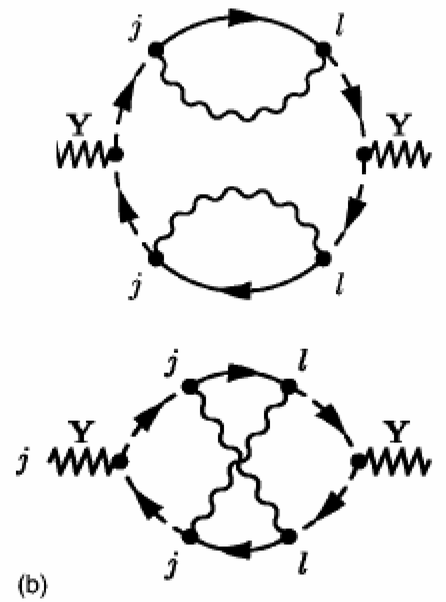

Correlation between Kondo Clouds

A

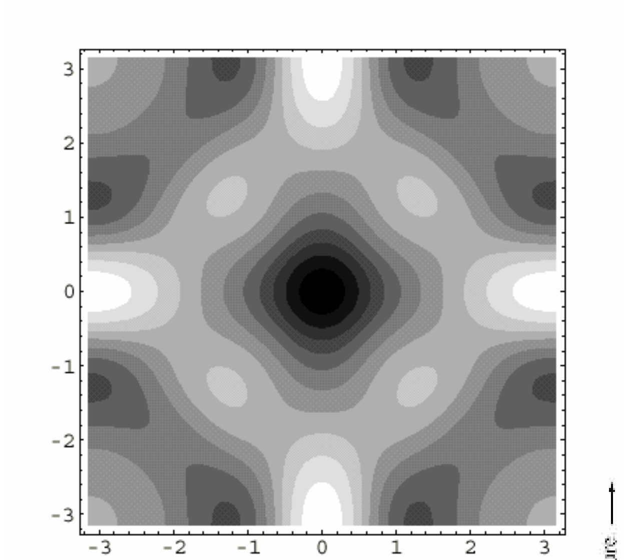

A) $2k_F R = \pi$

B) $2k_F R = 3\pi / 2$

B

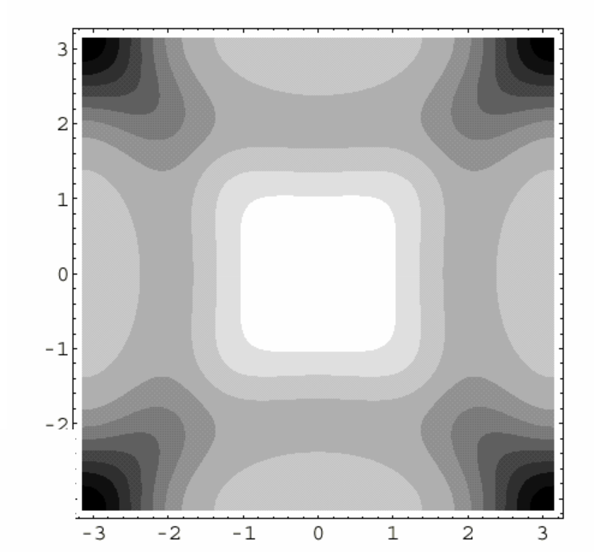

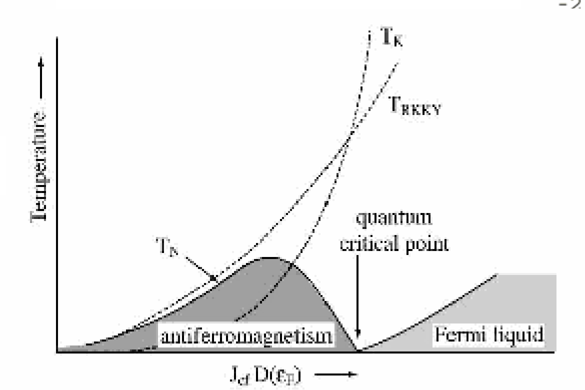

C

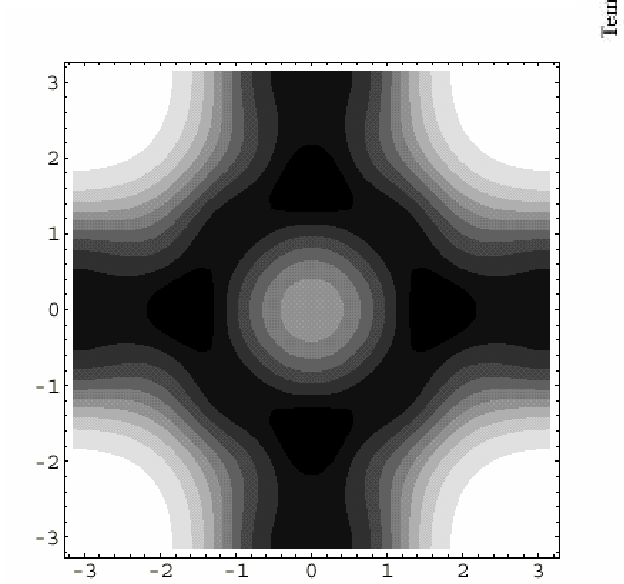

C) $2k_F R = 2\pi$

D) $2k_F R = 5\pi / 2$

D

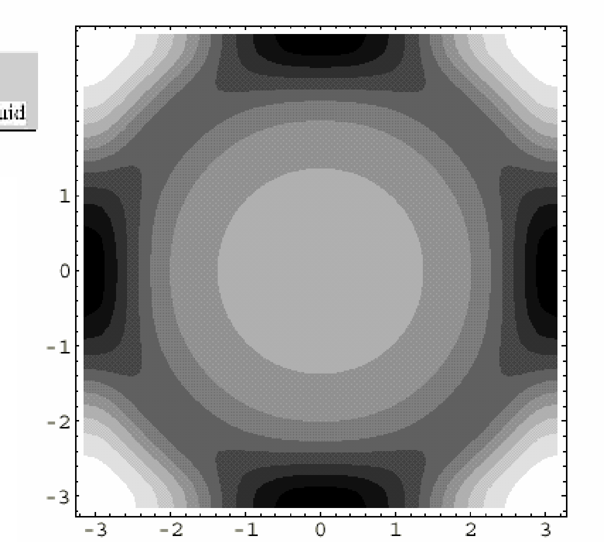

Conclusions

- Kondo screening suppresses magnetic and spin-glass transitions
- Kondo correlations enhance temperature of crossover to spin-liquid state
- Correlations between Kondo clouds result in non-universal temperature dependence of static magnetic susceptibility